

Discovering the constrained NMSSM with tau leptons at the LHC

Ulrich Ellwanger¹, Alice Florent², Dirk Zerwas²

¹ Laboratoire de Physique Théorique, UMR 8627, CNRS and Université Paris-Sud 11,
Bât. 210, F-91405 Orsay, France

² LAL, Université Paris-Sud 11, CNRS/IN2P3, Orsay, France

Abstract

The constrained Next-to-Minimal Supersymmetric Standard Model (cNMSSM) with mSugra-like boundary conditions at the GUT scale implies a singlino-like LSP with a mass just a few GeV below a stau NLSP. Hence, most of the squark/gluino decay cascades contain two τ leptons. The gluino mass $\gtrsim 1.2$ TeV is somewhat larger than the squark masses of $\gtrsim 1$ TeV. We simulate signal and background events for such a scenario at the LHC, and propose cuts on the transverse momenta of two jets, the missing transverse energy and the transverse momentum of a hadronically decaying τ lepton. This dedicated analysis allows to improve on the results of generic supersymmetry searches for a large part of the parameter space of the cNMSSM. The distribution of the effective mass and the signal rate provide sensitivity to distinguish the cNMSSM from the constrained Minimal Supersymmetric Standard Model in the stau-coannihilation region.

1 Introduction

The Next-to-Minimal Supersymmetric Standard Model (NMSSM, for recent reviews see [1, 2]) provides an elegant solution to the μ -problem of the Minimal Supersymmetric Standard Model (MSSM) [3]: after the replacement of the μ -term in the superpotential of the MSSM by the coupling to a gauge singlet superfield S , the superpotential is scale invariant and the only dimensionful parameters in the Lagrangian are soft Supersymmetry (SUSY) breaking terms.

After electroweak symmetry breaking, all components of the gauge singlet superfield S mix with the components of the MSSM-like Higgs doublet superfields H_u and H_d . Accordingly NMSSM specific phenomena can take place in the CP-even Higgs sector, the CP-odd Higgs sector and the neutralino sector. In this paper we concentrate on the neutralino sector, where the 5th singlet-like neutralino (in addition to the two neutral higgsinos, the neutral wino and the bino) can be the Lightest Supersymmetric Particle (LSP) [4–8] and, simultaneously, give rise to a dark matter density in agreement with WMAP constraints [9–14].

Such a scenario is not far fetched: A conceptually simple origin of soft SUSY breaking terms is a minimal coupling to supergravity (with a flavour independent Kähler potential and minimal gauge kinetic terms), and the assumption of spontaneously broken SUSY in a hidden sector. Then, the soft SUSY breaking terms are universal at the Planck scale (not far from the GUT scale) in the form of universal scalar masses m_0 , universal gaugino masses $M_{1/2}$ and universal trilinear scalar couplings proportional to A_0 .

The correspondingly constrained NMSSM (cNMSSM) has been studied first in [15–20]. Since then, the precision of the radiative corrections has been considerably improved, and the computation of the dark matter relic density has become possible [9]. Imposing the requirement of a dark matter relic density in agreement with WMAP constraints [14] as well as present constraints on Higgs and supersymmetric particle (sparticle) masses, the parameter space of the cNMSSM has been analysed recently in [21, 22]. (For studies of the semi-constrained NMSSM, where the singlet-dependent SUSY breaking parameters are allowed to be non-universal, see [12, 13, 23–25].)

Within the cNMSSM, the dark matter constraints require a singlino-like LSP. The origin of this phenomenon is quite easy to understand: first, the CP-even scalar singlet s has to assume a non-vanishing vacuum expectation value (vev) in order to generate the required μ -term. For this reason its SUSY breaking mass squared m_S^2 at the electroweak scale must not be very large; otherwise the minimum of its potential is at $s = 0$. Second, m_S^2 is hardly renormalized between the GUT and the electroweak scales, which leads to $m_S^2 \sim m_0^2$ with the consequence that, in the cNMSSM, m_0 must be small compared to $M_{1/2}$ and A_0 .

It is well known that, within the cMSSM [26], a small value of m_0 would imply a stau ($\tilde{\tau}_1$) LSP, which is not a reasonable candidate for the dark matter. In the cNMSSM, the singlino-like neutralino χ_1^0 can – and must – be lighter than the $\tilde{\tau}_1$ for this reason. In order for its dark matter relic density not being too large, its mass must be only a few GeV below the mass of the $\tilde{\tau}_1$ such that $\chi_1^0 - \tilde{\tau}_1$ coannihilation processes are sufficiently fast [12, 21, 22].

Such a scenario would necessarily have a strong impact on sparticle searches at colliders (see [27, 28] for reviews of searches at the LHC): since the $\tilde{\tau}_1$ is the NLSP and the singlino-like neutralino χ_1^0 couples only very weakly to all sparticles, the sparticles decay first into the $\tilde{\tau}_1$ under the emission of at least one τ -lepton. Subsequently the $\tilde{\tau}_1$ decays into $\chi_1^0 + \tau$, hence each sparticle decay cascade contains typically two τ -leptons. In the present paper we study, for the first time, the corresponding implications for sparticle searches at the LHC.

As discussed in [21, 22], the sparticle (and Higgs) spectrum is quite constrained in the cNMSSM, and can essentially be parametrized by $M_{1/2}$. The present lower bounds on $m_{\tilde{\tau}_1}$ and the lower LEP bound of ~ 114 GeV on the CP-even Standard Model like Higgs mass require $M_{1/2} \gtrsim 520$ GeV which, in spite of $m_0 \lesssim 50$ GeV, implies a quite heavy sparticle spectrum: squark masses $\gtrsim 1$ TeV (apart from the somewhat lighter stop and sbottom masses), and a gluino mass $\gtrsim 1.2$ TeV. Since consequently squark production will be relatively frequent compared to gluino production (in fact, squark + gluino production dominates), the signal events will mostly lead to two jets (not counting ISR and FSR) with a quite large p_T as well as a large missing transverse energy E_T^{miss} . The sum of the squark and/or gluino production cross sections is, however, just ~ 1 pb or less (for larger $M_{1/2}$).

Each sparticle production event in the cNMSSM will contain typically four τ -leptons in the final state: two of the τ -leptons (those originating from $\tilde{\tau}_1$ decays into $\chi_1^0 + \tau$) will be quite soft due to the small $\tilde{\tau}_1 - \chi_1^0$ mass difference $\lesssim 5$ GeV and are difficult to detect, whereas the τ -leptons from decays as $\chi_2^0 \rightarrow \tilde{\tau}_1 + \tau$ are relatively energetic.

The aim of the present paper is to show that a dedicated analysis allows for much better signal to background ratios for the cNMSSM than standard (generic) supersymmetric analyses. We simulate and study signals and various Standard Model backgrounds for the LHC at 14 TeV c.m. energy, and find that the signal to background ratio is sufficiently large allowing for the discovery of the cNMSSM for a wide range of values of $M_{1/2}$.

Events with E_T^{miss} , jets and τ -leptons could also be a signal for the (c)MSSM in the so-called stau-coannihilation region [29–33]. Since the squark/neutralino spectrum of the cMSSM is necessarily different from the cNMSSM, the combination of M_{eff} (essentially the sum of the transverse momenta and E_T^{miss}) and the signal rate has sensitivity to distinguish the two models.

In the next section we present the spectrum of the cNMSSM. In section 3 we discuss the signal, backgrounds and appropriate cuts. Details of the simulation of the cNMSSM signal and the Standard Model backgrounds, the effect of cuts, and the resulting cross sections and signal to background ratios are given in section 4. Section 5 is devoted to the comparison of the cNMSSM with the cMSSM, and Section 6 to conclusions and an outlook.

2 The spectrum of the cNMSSM

The NMSSM with a scale invariant superpotential W [1, 2] differs from the MSSM through the replacement of the μ term in W_{MSSM} by the coupling to a gauge singlet superfield S and a trilinear S self-coupling:

$$W_{MSSM} = \mu H_u H_d + \dots \rightarrow W_{NMSSM} = \lambda S H_u H_d + \frac{\kappa}{3} S^3 + \dots, \quad (2.1)$$

where we have omitted the quark/lepton Yukawa couplings. Hence, if the vev s of S is non-zero (induced by the soft SUSY breaking terms), an effective μ term $\mu_{eff} = \lambda s$ of the desired order of magnitude is generated and solves the μ problem of the MSSM [3].

Apart from the Yukawa couplings in the superpotential and the gauge couplings, the Lagrangian of the NMSSM depends on soft SUSY breaking scalar masses for the Higgs fields H_u , H_d and S , the squarks and the sleptons; trilinear couplings among the scalars (proportional to the couplings in the superpotential); and gaugino masses for the bino (M_1), the winos (M_2) and the gluino (M_3). Assuming supersymmetry breaking from a hidden sector in minimal supergravity (mSUGRA), the SUSY breaking terms are assumed to be universal at the scale of grand unification (near the Planck scale) and denoted as m_0 , A_0 and $M_{1/2}$, respectively. Hence the parameters of the corresponding cNMSSM are, apart from the gauge and quark/lepton Yukawa couplings,

$$m_0, A_0, M_{1/2}, \lambda \text{ and } \kappa. \quad (2.2)$$

It is convenient to fix κ from the requirement that the Higgs vevs h_u and h_d generate the correct value of M_Z .

As mentioned in the introduction and discussed in detail in [21, 22], the remaining parameters in (2.2) are strongly constrained: m_0 must be small such that the vev s is non-zero. A small non-zero value for m_0 affects essentially only the singlet-like CP-even Higgs mass [22], which is irrelevant for the present study; hence we assume $m_0 = 0$ in the following. In order to avoid a $\tilde{\tau}_1$ LSP, the singlino (the fermionic component of S) must be lighter such that $\tilde{\tau}_1$ is the NLSP. The singlino relic density can be reduced to an amount compatible with WMAP constraints, if its co-annihilation rate with the $\tilde{\tau}_1$ is large enough, i.e. if the corresponding mass difference is sufficiently small. This fixes $A_0 \sim -\frac{1}{4}M_{1/2}$ [21, 22]. Finally λ must also be quite small, since λ induces mixings in the CP-even Higgs sector between the doublet- and singlet-like Higgs states: if the singlet-like Higgs state is heavier than the (Standard Model like) Higgs state h , the mass of h falls below the LEP bound of ~ 114 GeV if λ is too large; if the mass of singlet-like Higgs state is below m_h (below 114 GeV as for the point P520 in Table 1 below), its coupling to the Z boson violates again LEP bounds [34] for λ too large. All in all one finds $\lambda \lesssim 0.02$ [21, 22] (but $\lambda \gtrsim 10^{-5}$ in order still to allow for singlino- $\tilde{\tau}_1$ co-annihilation).

λ induces also mixings between the singlet-like neutralino and the MSSM-like neutralinos (bino, neutral wino and higgsinos). For $\lambda \lesssim 0.02$, these mixings are very small. Hence the couplings of the singlino-like LSP χ_1^0 to all MSSM-like sparticles (squarks, gluino, sleptons, charginos and neutralinos), which are induced by these mixings, are very small as well. Accordingly branching ratios of all these sparticles into the singlino-like LSP are negligibly small, unless a decay into χ_1^0 is the only decay possible. Due to R-parity conservation this is the case for the NLSP, the $\tilde{\tau}_1$. Hence sparticle decay cascades proceed as in the MSSM (with a spectrum as in the cNMSSM, but without the singlet-like states) until the $\tilde{\tau}_1$ NLSP is produced. Depending on λ , the width of the final decay $\tilde{\tau}_1 \rightarrow \chi_1^0 + \tau$ can be so small, that the $\tilde{\tau}_1$ decay vertex is visibly displaced [22]. This case (where the displaced vertex corresponds to the production of a soft τ -lepton) could be another interesting signature for the cNMSSM, but subsequently we will not assume that λ is so small that this phenomenon occurs.

Concerning the remaining parameter $M_{1/2}$, we find that the LEP constraints on the Higgs sector require $M_{1/2} \gtrsim 520$ GeV. Then, all bounds on sparticle masses from colliders as well as constraints from B-physics are satisfied. For the calculation of the spectrum we use the code NMSPEC [23] within NMSSMTools [35, 36], updated including radiative corrections to the Higgs sector from [37]. The dark matter relic density is computed with the help of micrOMEGAs [9]. Clearly, very large values of $M_{1/2}$ are generally disfavoured by fine-tuning arguments; moreover, smaller values of $M_{1/2} \lesssim 1$ TeV allow to explain the discrepancy of the measured anomalous magnetic moment of the muon with the Standard Model [22]. Subsequently we confine ourselves to $M_{1/2} \leq 1$ TeV. In Table 1 we show the values for A_0 , $\tan\beta = h_u/h_d$ and μ_{eff} (A_0 is determined by the correct dark matter relic density, whereas $\tan\beta$ and μ_{eff} are obtained as output) as well as the Higgs and sparticle spectra for $M_{1/2} = 520, 600, 800$ GeV and 1 TeV for $m_0 = 0$ and $\lambda = 0.001$.

We see that, as announced above, $m_{\tilde{\tau}_1} - m_{\chi_1^0} \lesssim 5$ GeV and hence τ -leptons from the decay $\tilde{\tau}_1 \rightarrow \chi_1^0 + \tau$ are necessarily soft. τ -leptons from the decay $\chi_2^0 \rightarrow \tilde{\tau}_1 + \tau$ (where χ_2^0 is dominantly bino-like) profit at least from $m_{\chi_2^0} - m_{\tilde{\tau}_1} \sim 70$ GeV (for P520), or more energy from the decays of other sparticles into $\tilde{\tau}_1$. Note that right-handed sleptons \tilde{e}_R and $\tilde{\mu}_R$ decay essentially via the three-body channel as $\tilde{e}_R \rightarrow e + \tilde{\tau}_1 + \tau$. In fact, apart from the NMSSM-specific decay $\tilde{\tau}_1 \rightarrow \chi_1^0 + \tau$ (with a branching ratio of 100 %), the corresponding sparticle decay branching ratios can be obtained from the code SUSY-HIT [38] and the MSSM with a corresponding spectrum, which is used for the simulations of events below.

At the LHC, the dominant sparticle production processes are of course squark-gluino and squark-(anti-)squark pair productions. Subsequently a typical squark decay cascade looks like

$$\tilde{q} \rightarrow q + \chi_2^0 \rightarrow q + \tau + \tilde{\tau}_1 \rightarrow q + \tau + \tau + \chi_1^0, \quad (2.3)$$

but many more possibilities exist. Their simulation, together with the simulation of Standard Model background processes, will be discussed in the next sections.

3 The signal, backgrounds and cuts

As for most SUSY models, the production of squarks of the first generation and of gluinos will be the dominant sparticle production processes at the LHC. Their total production cross sections are obtained at NLO (QCD) from PROSPINO [39], and are also shown in Table 1. The dominant contributions originate from squark + gluino production ($\sim 37\%$) and squark pair production ($\sim 25\%$); less dominant are squark + antisquark production ($\sim 13\%$) and gluino pair production ($\sim 5\%$). The production cross sections of stop and sbottom squarks, sleptons, charginos and neutralinos add another $\sim 19\%$ to the total sparticle production cross sections.

The dominant background processes for SUSY searches are well-known: top-antitop pair production, W+n-jet production, Z+n-jet production, W+Z production and WW+n-jet production. Since we will compare the performance of our simulation with the results of standard SUSY searches by ATLAS [40], we assume the same production cross sections for these background processes as in [40] (given in Table 2 below).

Given that gluinos (whose decay generates typically two hard jets) are even somewhat heavier than the first generation squarks (generating typically one hard jet), we require at

	P520	P600	P800	P1000
$M_{1/2}$ (GeV)	520	600	800	1000
A_0 (GeV)	-142	-166	-225	-282
$\tan \beta$	23.2	24.3	26.6	28.3
μ_{eff} (GeV)	666	757	977	1190
$m_{h_1^0}$ (GeV)	100	115	117	118
$m_{h_2^0}$ (GeV)	115	118	159	199
$m_{h_3^0}$ (GeV)	654	738	937	1127
$m_{a_1^0}$ (GeV)	174	203	275	345
$m_{a_2^0}$ (GeV)	654	738	937	1127
m_{h^\pm} (GeV)	667	751	951	1140
$m_{\chi_1^0}$ (GeV)	142	166	225	282
$m_{\chi_2^0}$ (GeV)	215	250	338	427
$m_{\chi_3^0}$ (GeV)	404	471	636	801
$m_{\chi_{4,5}^0}$ (GeV)	680	770	990	1200
$m_{\chi_1^\pm}$ (GeV)	404	471	636	801
$m_{\chi_2^\pm}$ (GeV)	684	773	992	1203
$m_{\tilde{g}}$ (GeV)	1192	1361	1777	2187
$m_{\tilde{u}_L}$ (GeV)	1082	1234	1607	1973
$m_{\tilde{u}_R}$ (GeV)	1044	1189	1546	1895
$m_{\tilde{d}_L}$ (GeV)	1085	1237	1609	1974
$m_{\tilde{d}_R}$ (GeV)	1040	1184	1539	1886
$m_{\tilde{t}_1}$ (GeV)	825	947	1246	1538
$m_{\tilde{t}_2}$ (GeV)	1032	1165	1492	1816
$m_{\tilde{b}_1}$ (GeV)	973	1109	1444	1772
$m_{\tilde{b}_2}$ (GeV)	1020	1158	1496	1826
$m_{\tilde{e}_L}$ (GeV)	347	399	527	654
$m_{\tilde{e}_R}$ (GeV)	196	224	296	368
$m_{\tilde{\nu}_\tau}$ (GeV)	338	391	521	650
$m_{\tilde{\tau}_1}$ (GeV)	147	171	229	286
$m_{\tilde{\tau}_2}$ (GeV)	353	403	525	647
$m_{\tilde{\nu}_\tau}$ (GeV)	332	383	509	633
σ (pb)	1.36	0.70	0.134	0.035

Table 1: Input parameters, $\tan \beta$, μ_{eff} and low-energy spectra for four points of the cNMSSM with $m_0 = 0$ and $\lambda = 0.001$. In the last line we give the total NLO cross sections for the production of all sparticles at the LHC.

least two hard jets per event only whereas in generic supersymmetric analyses usually four hard jets are required. On the other hand, given the large squark and gluino masses, we can require quite large transverse momenta of the jets as well as a large missing transverse

energy E_T^{miss} .

For the τ -leptons we consider their hadronic decays only. For their transverse momenta we require at least 30 GeV, which allows to assume an efficiency of $\sim 40\%$ [40] (and a τ -fake rate of jets of $\sim 1 - 2\%$). On the other hand, since only two among the four τ -leptons per event are sufficiently energetic and the total signal cross sections are already quite small, we require one identified τ -lepton only.

Additional standard cuts are a lower limit on the angle $\Delta\Phi$ between the hard jets and E_T^{miss} , as well as a cut on the transverse mass M_T formed from E_T^{miss} and the identified τ -lepton (in order to remove semileptonically decaying W+jets events). Altogether, the list of our cuts is given by:

1. At least two jets, one with $p_T > 300$ GeV and one with $p_T > 150$ GeV
2. $E_T^{\text{miss}} > 300$ GeV
3. At least one τ -lepton with $p_T > 30$ GeV
4. $\Delta\Phi(j_i, E_T^{\text{miss}}) > 0.2$ for the hard jets
5. $M_T > 100$ GeV, where M_T is computed from the visible momenta of the hardest τ -lepton and E_T^{miss} .

Below we will denote this set of cuts as cNMSSM analysis.

4 Simulation, signal and background rates

Both the signal and the top quark background were generated by PYTHIA 6.4 [41], which was in charge of generation and phase-space decays. PYTHIA performed the parton showering as well as the matching procedure according to the MLM prescription including initial and final state radiation. TAUOLA [43–45] was employed for the τ -decays. All other backgrounds (involving at least one W or Z-boson) were generated with ALPGEN [42]. In order to keep the statistics manageable, preselection cuts were applied on the ALPGEN samples. Since event generation was performed by leading order generators, the cross sections were scaled according to the NLO cross sections in Table 1 for the signal, as in [40] to the NLO+NLL calculation for top production, and to NLO (or NNLO level, where available) for electroweak boson(s) production.

For the detector simulation we employed AcerDet [46]. AcerDet is a fast detector simulation which provides a reasonable description of the performance of an LHC detector. The events generated by PYTHIA and ALPGEN+PYTHIA were all passed through AcerDet. AcerDet reconstructs jets, leptons and the missing transverse energy, it also labels the origin of the jets, e.g., those coming from a tau lepton. The efficiency and the corresponding background rejection for a working point of 40% τ identification efficiency were implemented at reconstruction level.

One of the issues to be checked is the energy of the reconstructed tau-jets. For this initial check we used PYTHIA to produce Z bosons and their subsequent decay to tau leptons. The hadron-hadron as well as the lepton-hadron final states were reconstructed

and compared to the results of the ATLAS collaboration presented in [40]. Reasonable agreement at the level of a few percent (about 3 GeV) was found.

A fast detector simulation as AcerDet will not be able to simulate the non-Gaussian tails, e.g., in the transverse missing energy distribution. Simulation and reconstruction results without full detector simulation and reconstruction are therefore not expected to be perfectly reproduced. To get a feeling of how well the background can be modeled with AcerDet, two signatures of Ref. [40] have been implemented and analysed in addition to the dedicated cNMSSM analysis: the four-jet SUSY search (4j0l) and the SUSY search with at least one tau in the final state (4jtau).

	Events	cross section (pb)	4j0l (fb)	4jtau (fb)	cNMSSM (fb)
tt	2110000	833	350±12	50±4.4	7.9±1.7
W+2jets	222700	281	0	0	0
W+3jets	89250	116	15±4.5	0	2.6±1.8
W+4jets(inc)	50875	61	220±16	9.6±3.4	4.8±2.4
W+jets (inc)			235±16.6	9.6±3.4	7.4±3
Z+2jets	88850	106	0	0	0
Z+3jets	22320	27.5	0	0	0
Z+4jets(inc)	11639	10.1	0.9±0.9	0	0
Z+jets			0.9±0.9	0	0
ZW(inc)	250	0.5	2±2	0	0
WW+0jet	50000	47	0	0	0
WW+1jet	15000	20	0	0	0
WW+2jet(inc)	32796	13	17.8±2.6	1.2±0.7	0.8±0.6
WW+jets (inc)			17.8±2.6	1.2±0.7	0.8±0.6
Total			606±21	61±5.6	16.1±3.5

Table 2: The number of simulated background events, cross sections before cuts, and cross sections after the 4j0l, 4jtau and the cNMSSM analysis. The quoted error is the statistical error.

In Table 2 the result of the background cross sections before and after the cuts is shown for the two ATLAS as well as the cNMSSM signatures. For the 4j0l analyses, the AcerDet-result for the total background cross section of about 606 fb after cuts is of the right order of magnitude compared to 708 fb (NLO) in [40]. Adding the tau identification to the analysis in the 4jtau analysis, a total background cross section of 61 fb after cuts obtained here is to be compared with 51 fb at NLO in [40]. Thus with and without tau identification, AcerDet provides a reasonable estimate of the expected background with respect to the dedicated full simulation.

We note that already with the softer cuts within the 4j0l analyses and notably the cuts on $\Delta\Phi(j_i, E_T^{\text{miss}})$, the remaining QCD background was found to be small in [40]. In our case, QCD events could pass the cNMSSM cuts only if a very large value of E_T^{miss} and a τ -lepton would be faked simultaneously. Assuming a jet $\rightarrow \tau$ fake rate up to $\sim 2\%$ (for an acceptance of 40%), and that the suppression rate of QCD events without missing energy for $E_T^{\text{miss}} > 150$ GeV is 1% [40] while we cut at 300 GeV, we should be safe of the QCD

background.

Whereas the two ATLAS analyses are designed to cover a large variety of supersymmetric signals, the signatures discussed above are chosen specifically for heavy squarks and gluinos as well as τ -rich final states as in the cNMSSM. The background cross sections for this analysis are shown in the last column of Table 2. The total background, already decreased from the 4-jet-0-lepton to the 4-jet-tau analysis by an order of magnitude, is reduced by another factor four to ~ 16 fb.

Typically the overall efficiency for all SUSY processes weighted by the cross section varies between 7% and 10%. The cross section for the cNMSSM benchmark points after all cuts are shown in Table 3 for the three analyses. The S/B ratio, the ratio S/\sqrt{B} for an integrated luminosity of 1 fb^{-1} as well as for 30 fb^{-1} are shown.

		4j0l	4jtau	cNMSSM
P520	1.36pb	$101 \pm 1.1\text{fb}$	$27 \pm 0.5\text{fb}$	$99 \pm 1\text{fb}$
S/B		0.17	0.44	6.2
S/\sqrt{B}	1 fb^{-1}	4.1	3.4	24.8
S/\sqrt{B}	30 fb^{-1}	22	19	136
P600	0.70pb	$47 \pm 0.5\text{fb}$	$13.3 \pm 0.3\text{fb}$	$58 \pm 0.6\text{fb}$
S/B		0.08	0.21	3.6
S/\sqrt{B}	1 fb^{-1}	1.9	1.7	14.5
S/\sqrt{B}	30 fb^{-1}	10.5	9.3	79
P800	0.134pb	$7.5 \pm 0.1\text{fb}$	$2.7 \pm 0.05\text{fb}$	$13.4 \pm 0.1\text{fb}$
S/B		0.012	0.04	0.8
S/\sqrt{B}	1 fb^{-1}	0.3	0.34	3.4
S/\sqrt{B}	30 fb^{-1}	1.7	1.9	18
P1000	0.035pb	$1.68 \pm 0.02\text{fb}$	$0.62 \pm 0.01\text{fb}$	$3.43 \pm 0.03\text{fb}$
S/B		0.002	0.01	0.2
S/\sqrt{B}	1 fb^{-1}	0.07	0.07	0.86
S/\sqrt{B}	30 fb^{-1}	0.37	0.43	4.7

Table 3: Signal expectation for the NMSSM points at NLO after all cuts for the benchmark points. At least 120000 events per point were generated. The error is the statistical error. For every point the ratios S/B and S/\sqrt{B} for an integrated luminosity of 1 fb^{-1} and 30 fb^{-1} are shown.

Table 3 clarifies the advantage of the cNMSSM cuts with respect to the general analysis: the ratio S/\sqrt{B} is 7–10 times larger for the cNMSSM cuts even with respect to the standard 4-jet-tau signature, which originates both from the larger background suppression and the larger efficiency on the signal. Correspondingly the cNMSSM cuts allow for a sensitivity, for a given luminosity, on a much larger part of the cNMSSM parameter space (for heavier squarks/gluinos). The point P800 (with squark/gluino masses of 1.6/1.7 TeV) is hardly visible within the standard analysis even for 30 fb^{-1} , whereas the ratio S/\sqrt{B} is still ~ 18 for the cNMSSM cuts. Only for the point P1000 (with squark/gluino masses of 1.9/2.2 TeV) a larger luminosity and/or even harder cuts seem to be required for detection.

In Figure 1 we show the spectrum of the effective mass $M_{\text{eff}} \equiv \sum p_{\text{T}}^{\text{jets}} + \sum p_{\text{T}}^{\text{lep}} + E_{\text{T}}^{\text{miss}}$ after all cuts of the cNMSSM analysis are applied, normalised to an integrated luminosity of 1 fb^{-1} . Typically, the spectrum of the effective mass peaks at a value corresponding to the masses of the pair produced sparticles [40]. Here the maxima of M_{eff} are shifted to somewhat larger values due to the cuts on $p_{\text{T}}^{\text{jets}}$ and $E_{\text{T}}^{\text{miss}}$. As expected, the spectrum of M_{eff} is harder for the points with heavier squarks/gluinos.

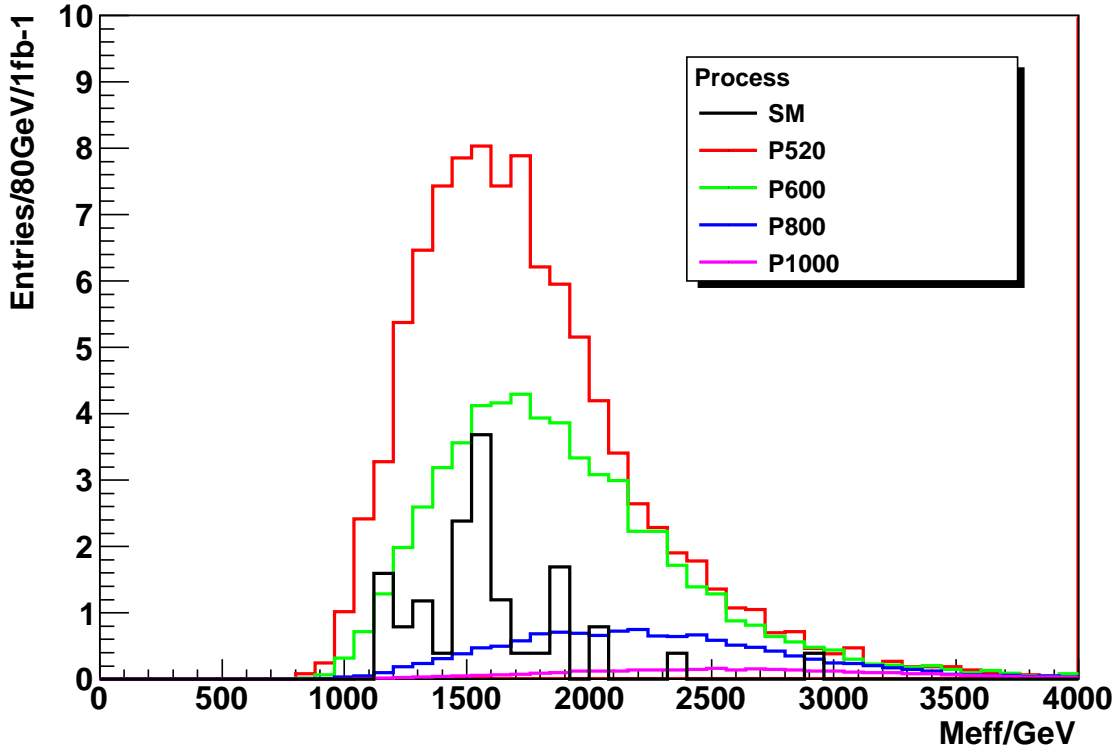


Figure 1: The effective mass distribution for the SM background and the cNMSSM points from Table 1, after all cuts of the cNMSSM analysis are applied, normalised to an integrated luminosity of 1 fb^{-1} .

For completeness we show in Figure 2 the transverse momentum of the leading tau candidate (after the cNMSSM cuts). Modulo the rate, the spectrum of the leading tau candidate is slightly harder for the points with heavier squarks/gluinos.

5 Comparison with the cMSSM in the stau coannihilation region

It is well-known that τ -rich final states from squark or gluino production would also be generated in the so-called stau coannihilation region of the (c)MSSM [29–33]. Hence the question arises, by which signatures this region of the cMSSM can be distinguished from the cNMSSM.

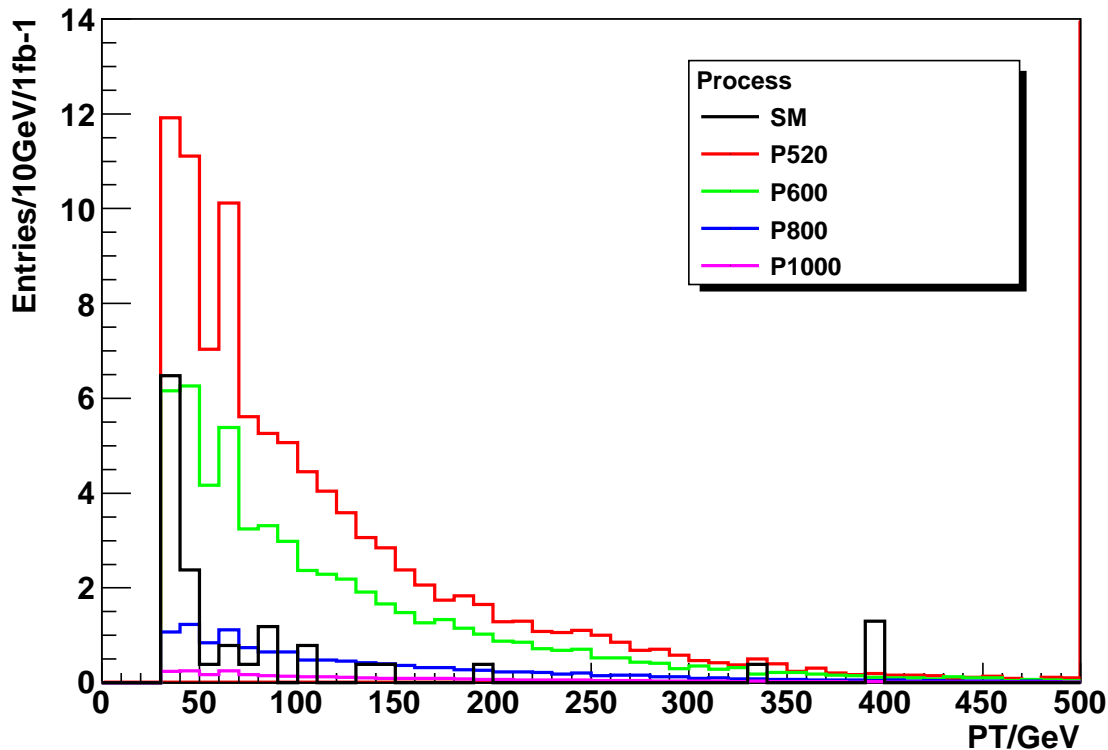


Figure 2: The transverse momentum distribution of the leading tau after all cuts of the cNMSSM analysis are applied, normalised to an integrated luminosity of 1 fb^{-1} .

Clearly, the neutralino/ $\tilde{\tau}$ spectrum of the cMSSM is different from the one of the cNMSSM: in the cMSSM (in the stau coannihilation region, which we assume henceforth) the lighter $\tilde{\tau}_1$ has a mass close to the bino-like neutralino LSP χ_1^0 , whereas the neutralino χ_2^0 is typically wino-like. At first sight, a squark decay cascade as in Eq.(2.3) is also possible within the cMSSM, with corresponding replacements of the neutralinos χ_1^0 and χ_2^0 . However, all right-handed squarks (and sleptons) would not couple to the wino-like χ_2^0 , and prefer to decay directly into the bino-like χ_1^0 . These decays do *not* lead to two τ -leptons in the cascade. As a consequence, the τ -rich cascades hardly occur for right-handed squark decays, and are thus less frequent (relative to the total squark production cross section) than in the cNMSSM.

On the other hand, squarks and gluinos can be considerably lighter in the cMSSM than in the cNMSSM, since smaller values of $M_{1/2}$ – together with larger non-zero values of m_0 – are allowed. In particular this is the case, if we look for a point in the cMSSM parameter space with similar χ_1^0 and $\tilde{\tau}_1$ masses as the point P520 of the cNMSSM. It turns out that, for the corresponding values of $M_{1/2}$ and m_0 (we take $A_0 = 0$ for simplicity), the squarks and gluinos are considerably lighter than for the point P520. Hence we denote this point as MSSMl (“l” for “light”). Its parameters and sparticle masses are given in Table 4 below.

As indicated in the last line in Table 4, the lighter squarks and gluinos imply considerably larger production cross sections for the point MSSMl compared to P520. As a consequence,

	MSSMl	MSSMh
$M_{1/2}$ (GeV)	360	520
m_0 (GeV)	210	200
A_0 (GeV)	0	0
$\tan \beta$	40	30
μ_{eff} (GeV)	466	649
$m_{h_1^0}$ (GeV)	114	117
$m_{\chi_1^0}$ (GeV)	146	215
$m_{\chi_2^0}$ (GeV)	274	406
$m_{\chi_{3,4}^0}$ (GeV)	480	660
$m_{\chi_1^\pm}$ (GeV)	274	406
$m_{\chi_2^\pm}$ (GeV)	486	666
$m_{\tilde{g}}$ (GeV)	851	1191
$m_{\tilde{u}_L}$ (GeV)	800	1100
$m_{\tilde{u}_R}$ (GeV)	776	1062
$m_{\tilde{d}_L}$ (GeV)	804	1103
$m_{\tilde{d}_R}$ (GeV)	774	1058
$m_{\tilde{t}_1}$ (GeV)	598	843
$m_{\tilde{t}_2}$ (GeV)	765	1038
$m_{\tilde{b}_1}$ (GeV)	688	984
$m_{\tilde{b}_2}$ (GeV)	749	1033
$m_{\tilde{e}_L}$ (GeV)	322	401
$m_{\tilde{e}_R}$ (GeV)	252	280
$m_{\tilde{\nu}_\tau}$ (GeV)	312	393
$m_{\tilde{\tau}_1}$ (GeV)	156	222
$m_{\tilde{\tau}_2}$ (GeV)	332	405
$m_{\tilde{\nu}_\tau}$ (GeV)	294	382
σ (pb)	9.44	1.40

Table 4: SUSY breaking parameters, $\tan \beta$, μ_{eff} , sparticle spectra and total sparticle cross sections for the cMSSM points MSSMl and MSSMh.

the number of events passing our cNMSSM analysis above is larger than for P520, in spite of the absence of τ -leptons in right-handed squark decays.

There exist also points in the cMSSM parameter space where the squark and gluino spectrum resembles the one of P520, implying similar production cross sections. Such points correspond to larger values of $M_{1/2}$ and m_0 ; an example is given by the point MSSMh (“h” for “heavy”), whose squark and gluino masses are similar to those of the cNMSSM point P520 (see Table 4).

The signal rates after the cNMSSM cuts for the points MSSMl and MSSMh are given in Table 5: these are considerably larger (as compared to P520) for the point MSSMl, but smaller for the point MSSMh in spite of the similar squark/gluino masses and hence the

similar total sparticle cross section (see Table 4). The reason was mentioned above: right-handed squarks do not decay via τ -rich cascades and, hence, right-handed squark decays do not contribute to the signal after the cNMSSM analysis.

		4j0l	4jtau	cNMSSM analysis
MSSMl	9.4pb	1429 \pm 10fb	121 \pm 3fb	166 \pm 4fb
S/B		2.4	2.0	10
S/ \sqrt{B}	1 fb $^{-1}$	58	15	42
S/ \sqrt{B}	30 fb $^{-1}$	320	84	227
MSSMh	1.40pb	242 \pm 1.7fb	22 \pm 0.5fb	41 \pm 0.7fb
S/B		0.4	0.46	2.5
S/ \sqrt{B}	1 fb $^{-1}$	9.8	2.8	10
S/ \sqrt{B}	30 fb $^{-1}$	54	15	56

Table 5: Signal expectation for the MSSM points at NLO after all cuts. 120000 events per point minimum were generated. The error is the statistical error.

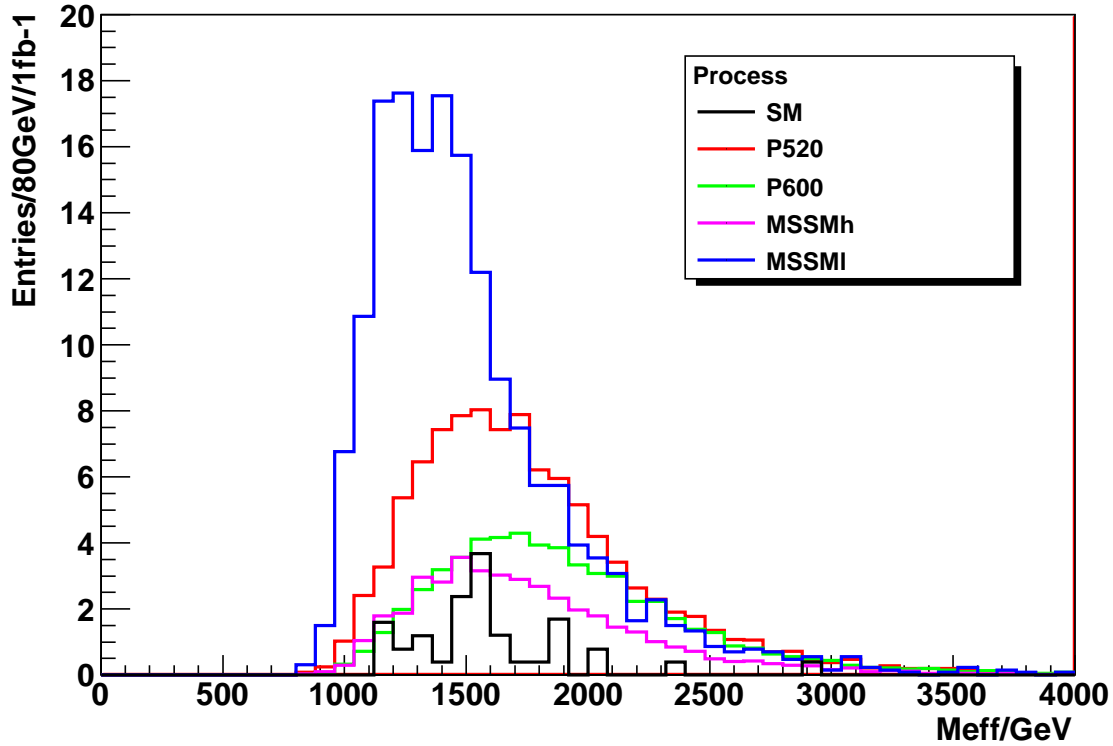


Figure 3: The effective mass distribution for the points P520, P600, MSSMl and MSSMh after all cuts of the cNMSSM analysis are applied.

The M_{eff} spectrum for the MSSM points, together with P520, P600 and the SM background, is shown in Fig. 3. First, the point MSSMl (with similar χ_1^0 and $\tilde{\tau}_1$ masses as the

point P520) has not only a larger signal cross section as compared to P520, but we see that its maximum of M_{eff} is visibly shifted towards smaller values.

Can we distinguish the point MSSMh from any of the cNMSSM points? Due to the similar squark/gluino masses as P520, MSSMh has its maximum of M_{eff} in the same region as P520, but a significantly smaller signal rate. The signal rate for the cNMSSM point P600 of about 58 fb is still larger than 41 fb for MSSMh. (The difference is slightly larger than a conservative error of 20-30% on the theoretical cross section prediction.) On the other hand we see in Fig. 3 that the maximum of M_{eff} for P600 is shifted towards larger values due to the heavier squarks/gluinos: the root mean square of the distributions is about 500 GeV and the difference of the average effective mass is about 130 GeV, so that the error on the average effective mass for 1 fb^{-1} is about 70 GeV, i.e., about two times smaller than the difference. The average effective mass is affected somewhat by the tails for large effective mass. Using a simple fit of the distributions, the peak to peak difference increases slightly to about 150 GeV providing for a stronger separation of MSSMh and P600. Any cNMSSM point with still heavier squarks/gluinos (such that the signal rate coincides with the one for MSSMh) will imply a maximum for still larger values of M_{eff} . Hence, the cNMSSM points have either measurably larger signal rates after applying the cNMSSM cuts (if the maxima of M_{eff} coincide with a MSSM point), or maxima at measurably larger values of M_{eff} (if the signal rates coincide with a MSSM point).

Additionally one can compare the cross section ratios after the generic supersymmetric 4j0l cut, which are 242 fb (MSSMh, where squarks are somewhat lighter than gluinos) as compared to 47 fb (P600, where gluinos are somewhat heavier than squarks). Hence, given a corresponding signal in the data, a careful comparison of both the signal rates for generic and dedicated searches and the maximum of M_{eff} (possibly including in addition the transverse momentum of the tau lepton) should allow to distinguish the cNMSSM from the MSSM in the stau coannihilation region.

6 Conclusions and outlook

In the present paper we have proposed criteria for the search for the fully constrained NMSSM at the LHC. In view of the relatively heavy squarks and gluinos in the cNMSSM and correspondingly small production cross sections, this task is not quite trivial. On the other hand, due to the large number of τ -leptons in the final states, signatures involving hadronic τ decays are relatively efficient. Whereas the soft τ -leptons in the final states are difficult to use, the requirement of at least one hard τ -lepton has a relatively large signal acceptance.

Combining this requirement with relatively hard cuts on the transverse momenta of two jets and $E_{\text{T}}^{\text{miss}}$ as specified at the end of section 3, the signal to background ratio is significantly improved with respect to the more standard 4j0l or 4jtau analyses. This result was obtained after simulations including detector effects and a τ acceptance, which we compared with and checked against the analysis of SUSY signals by the ATLAS group. Hence, already an integrated luminosity of 1 fb^{-1} (at 14 TeV c.m. energy) becomes sensitive to part of the parameter space of the cNMSSM whereas, trivially, more luminosity is required in case of heavier squarks and gluinos. In any case we believe that the cuts proposed here

are the most sensitive ones to the parameter space of the cNMSSM. In addition we have discussed in how far a refined analysis employing both the signal rate and the maximum of M_{eff} allows to distinguish the cNMSSM from the MSSM in the stau coannihilation region.

In the near future the LHC is on track to accumulate an integrated luminosity of 1 fb^{-1} at 7 TeV c.m. energy at the end of 2011. We have estimated the number of signal events for the point P520, if we lower the cNMSSM cuts correspondingly: for two jets we require $p_T > 50$ and 20 GeV, respectively, and $E_T^{\text{miss}} > 200$ GeV. We obtain about 5 signal events passing these cuts.

For our analysis of signals of the cNMSSM at 14 TeV c.m. energy we have left aside the presence of two soft τ leptons per event which represent, in principle, a spectacular signature for this class of models. In some regions of the parameter space of the cNMSSM – for very small values of λ and/or a small $\tilde{\tau}_1 - \chi_1^0$ mass difference – the life time of $\tilde{\tau}_1$ can be very small leading to displaced vertices of the decay $\tilde{\tau}_1 \rightarrow \tau + \chi_1^0$ into these soft τ -leptons. Using dedicated track-based algorithms, the search for these soft τ -leptons originating from displaced vertices is perhaps not completely hopeless.

In the framework of the general NMSSM, a singlino-like LSP can be accompanied by a NLSP different from $\tilde{\tau}_1$. The signatures of these scenarios would be very different from the ones discussed here (depending on the nature of the NLSP), and should also be investigated in the future.

Acknowledgments

We would like to thank T. Plehn and P. Wienemann for numerous discussions, K. Mawatari for help in interfacing PYTHIA with TAUOLA for supersymmetric models, and Sebastien Binet (LAL) for his invaluable help in automizing the production of the Alpgen samples. U.E. wishes to thank the Institut für Theoretische Physik in Heidelberg, where this work was started, for hospitality.

References

- [1] M. Maniatis, Int. J. Mod. Phys. A **25** (2010) 3505 [arXiv:0906.0777 [hep-ph]].
- [2] U. Ellwanger, C. Hugonie and A. M. Teixeira, Phys. Rept. **496** (2010) 1 [arXiv:0910.1785[hep-ph]].
- [3] J. E. Kim and H. P. Nilles, Phys. Lett. B **138** (1984) 150.
- [4] S. A. Abel, S. Sarkar and I. B. Whittingham, Nucl. Phys. B **392** (1993) 83 [arXiv:hep-ph/9209292].
- [5] U. Ellwanger and C. Hugonie, Eur. Phys. J. C **5** (1998) 723 [arXiv:hep-ph/9712300].
- [6] U. Ellwanger and C. Hugonie, Eur. Phys. J. C **13** (2000) 681 [arXiv:hep-ph/9812427].
- [7] S. Hesselbach, F. Franke and H. Fraas, Phys. Lett. B **492** (2000) 140 [arXiv:hep-ph/0007310].

- [8] V. Barger, P. Langacker and G. Shaughnessy, Phys. Lett. B **644** (2007) 361 [arXiv:hep-ph/0609068].
- [9] G. Belanger, F. Boudjema, C. Hugonie, A. Pukhov and A. Semenov, JCAP **0509** (2005) 001 [arXiv:hep-ph/0505142].
- [10] J. F. Gunion, D. Hooper and B. McElrath, Phys. Rev. D **73** (2006) 015011 [arXiv:hep-ph/0509024].
- [11] D. G. Cerdeno, E. Gabrielli, D. E. Lopez-Fogliani, C. Munoz and A. M. Teixeira, JCAP **0706** (2007) 008 [arXiv:hep-ph/0701271].
- [12] C. Hugonie, G. Belanger and A. Pukhov, JCAP **0711** (2007) 009 [arXiv:0707.0628 [hep-ph]].
- [13] G. Belanger, C. Hugonie and A. Pukhov, JCAP **0901** (2009) 023 [arXiv:0811.3224 [hep-ph]].
- [14] E. Komatsu *et al.* [WMAP Collaboration], Astrophys. J. Suppl. **180** (2009) 330 [arXiv:0803.0547 [astro-ph]].
- [15] J. R. Ellis, J. F. Gunion, H. E. Haber, L. Roszkowski and F. Zwirner, Phys. Rev. D **39** (1989) 844.
- [16] M. Drees, Int. J. Mod. Phys. A **4** (1989) 3635.
- [17] U. Ellwanger, M. Rausch de Traubenberg and C. A. Savoy, Phys. Lett. B **315** (1993) 331 [arXiv:hep-ph/9307322].
- [18] T. Elliott, S. F. King and P. L. White, Phys. Lett. B **351** (1995) 213 [arXiv:hep-ph/9406303].
- [19] S. F. King and P. L. White, Phys. Rev. D **52** (1995) 4183 [arXiv:hep-ph/9505326].
- [20] U. Ellwanger, M. Rausch de Traubenberg and C. A. Savoy, Nucl. Phys. B **492** (1997) 21 [arXiv:hep-ph/9611251].
- [21] A. Djouadi, U. Ellwanger and A. M. Teixeira, Phys. Rev. Lett. **101** (2008) 101802 [arXiv:0803.0253 [hep-ph]].
- [22] A. Djouadi, U. Ellwanger and A. M. Teixeira, JHEP **0904** (2009) 031 [arXiv:0811.2699 [hep-ph]].
- [23] U. Ellwanger and C. Hugonie, Comput. Phys. Commun. **177** (2007) 399 [arXiv:hep-ph/0612134].
- [24] A. Djouadi *et al.*, JHEP **0807** (2008) 002 [arXiv:0801.4321 [hep-ph]].
- [25] C. Balazs and D. Carter, Phys. Rev. D **78** (2008) 055001 [arXiv:0808.0770 [hep-ph]].

- [26] D. J. H. Chung, L. L. Everett, G. L. Kane, S. F. King, J. D. Lykken and L. T. Wang, Phys. Rept. **407** (2005) 1 [arXiv:hep-ph/0312378].
- [27] D. E. Morrissey, T. Plehn, T. M. P. Tait, [arXiv:0912.3259 [hep-ph]].
- [28] P. Nath, B. Nelson, H. Davoudiasl *et al.*, Nucl. Phys. Proc. Suppl. **200-202** (2010) 185-417. [arXiv:1001.2693 [hep-ph]].
- [29] J. R. Ellis, T. Falk and K. A. Olive, Phys. Lett. B **444** (1998) 367 [arXiv:hep-ph/9810360].
- [30] J. A. Aguilar-Saavedra *et al.*, Eur. Phys. J. C **46** (2006) 43 [arXiv:hep-ph/0511344].
- [31] R. L. Arnowitt, B. Dutta, T. Kamon, N. Kolev and D. A. Toback, Phys. Lett. B **639** (2006) 46 [arXiv:hep-ph/0603128].
- [32] U. Chattopadhyay, D. Das, A. Datta and S. Poddar, Phys. Rev. D **76** (2007) 055008 [arXiv:0705.0921 [hep-ph]].
- [33] R. L. Arnowitt, B. Dutta, A. Gurrola, T. Kamon, A. Krislock and D. Toback, Phys. Rev. Lett. **100** (2008) 231802 [arXiv:0802.2968 [hep-ph]].
- [34] S. Schael *et al.* [ALEPH and DELPHI and L3 and OPAL Collaborations and LEP Working Group for Higgs Boson Searches], Eur. Phys. J. C **47** (2006) 547 [arXiv:hep-ex/0602042].
- [35] U. Ellwanger, J. F. Gunion and C. Hugonie, JHEP **0502** (2005) 066 [arXiv:hep-ph/0406215].
- [36] U. Ellwanger and C. Hugonie, Comput. Phys. Commun. **175** (2006) 290 [arXiv:hep-ph/0508022].
- [37] G. Degrandi and P. Slavich, Nucl. Phys. B **825** (2010) 119 [arXiv:0907.4682 [hep-ph]].
- [38] A. Djouadi, M. M. Muhlleitner and M. Spira, Acta Phys. Polon. B **38** (2007) 635 [arXiv:hep-ph/0609292].
- [39] W. Beenakker, R. Hopker and M. Spira, "PROSPINO: A program for the PROduction of Supersymmetric Particles In Next-to-leading Order QCD," arXiv:hep-ph/9611232, for updates see <http://www.thphys.uni-heidelberg.de/~plehn/prospino/>
- [40] G. Aad *et al.* [The ATLAS Collaboration], arXiv:0901.0512 [hep-ex].
- [41] T. Sjostrand, S. Mrenna and P. Z. Skands, JHEP **0605** (2006) 026 [arXiv:hep-ph/0603175].
- [42] M. L. Mangano, M. Moretti, F. Piccinini, R. Pittau and A. D. Polosa, JHEP **0307**, 001 (2003) [arXiv:hep-ph/0206293].
- [43] S. Jadach, J. H. Kuhn and Z. Was, Comput. Phys. Commun. **64** (1990) 275.

- [44] M. Jezabek, Z. Was, S. Jadach and J. H. Kuhn, *Comput. Phys. Commun.* **70** (1992) 69.
- [45] S. Jadach, Z. Was, R. Decker and J. H. Kuhn, *Comput. Phys. Commun.* **76** (1993) 361.
- [46] E. Richter-Was, arXiv:hep-ph/0207355.